Concentration Dependence of the Interfacial Depletion Layer Thickness for Polymer Solutions in Contact with Nonadsorbing Walls

D. Ausserre, H. Hervet, and F. Rondelez*

Physique de la Matière Condensée, Collège de France, 75231 Paris Cedex 05, France.
Received March 11, 1985

ABSTRACT: We have investigated optically the thickness e of the depletion layer induced in xanthan aqueous polymer solutions by the presence of a nonadsorbing, fused-silica wall. The measurements have been performed at several bulk polymer concentrations Φ_b. We observe that e, defined from the surface excess Γ as $e = \Gamma/\Phi_b$, stays comparable with the radius of gyration R_G up to the crossover concentration Φ_b^* to the semidilute regime. Above Φ_b^*, e becomes a decreasing function of Φ_b and scales approximately as $e \sim \Phi_b^x$ with $x = -0.79 \pm 0.10$, in agreement with the de Gennes prediction for flexible chains ($x = -0.75$). This result stresses the fact that stiff macromolecules such as xanthan still exhibit properties typical of flexible coils provided the spatial scale of observation is larger than the intrinsic persistence length of the chain.

Introduction

In the vicinity of a solid–liquid interface, the properties of polymer solutions are strongly modified relative to the properties exhibited by the same solution in an unrestricted (bulk) volume. These barrier-induced changes affect the equilibrium properties by creating a nonuniform monomer concentration profile near the wall.[1] They also affect the dynamic behavior by hampering some of the monomer motions.[2] Much work has been devoted over the years to the understanding of these rather subtle problems. However, it is only fair to say that the theoretical studies have by far outnumbered the experiments.[3] The main reason for that situation is the difficulty involved in the measurements of minute polymer concentrations over submicroscopic distances. Apart from their interest in their own right, such studies are stimulated by the importance of the polymer–solid substrate interactions in such technologically important fields as colloid stabilization, adhesion, surface protection, lubrication, chromatography, and enhanced oil recovery.[4]

In two recent reports[5,6] we have shown how the EWIF optical technique (EWIF is the acronym for "evanescent wave-induced fluorescence") provides a powerful experimental tool to study the monomer concentration profile in the interfacial layer of polymer solutions near a flat, transparent, solid wall. We have always considered impenetrable but otherwise passive barriers, i.e., neither adsorbing nor long-range repulsive. In that case, theory predicts that the chains experience a strong entropic repulsion if the distance between their center of mass and the wall gets smaller than a characteristic length related to their overall size.[7] Consequently a depletion layer is formed in which the local polymer density Φ is markedly lower than the bulk concentration Φ_b. In ref 5, we measured the overall thickness of the depletion layer for a dilute solution of short flexible polystyrene chains ($M_w \simeq 10^5$) and found it to be comparable with the chain radius of gyration. In ref 6, using stiff xanthan chains of relatively high molecular weight ($M_w \simeq 1.8 \times 10^6$), we were able to measure the full monomer concentration profile within the depletion layer. Xanthan was a good system to work with because of its relatively long intrinsic persistence length, which brings the thickness of the interfacial layer well above the minimum spatial scale probed by the EWIF technique. However, the results could not quite distinguish between two fairly different models: (1) the fully rigid-rod profile proposed by Auvray,[8] using an equivalent rod length equal to the known end-to-end distance for the chain; (2) a mixed "rigid then flexible" profile, in which the chain is considered to be rigid for all distances shorter than the chain persistence length and flexible for all larger distances.

All of the above experiments have been conducted in dilute solutions. In the present study we investigate the influence of the bulk polymer concentration on the interfacial properties of xanthan chains in contact with a nonadsorbing fused-silica wall. We will see that the thickness of the depletion layer e stays constant until the concentration of first overlap between the chains is eventually reached. For still larger concentrations, e becomes a decreasing function of the bulk polymer concentration. These observations are in agreement with the predictions of Joanny, Leibler, and de Gennes[3] and Fleer, Scheutjens, and Vincent[15] for flexible chains in the semidilute regime. According to ref 3, e is proportional to the correlation length $\xi(\Phi)$ describing the spatial range over which the monomer–monomer density correlation function relaxes back to its average bulk value. In turn this proves that chains with finite persistence lengths such as xanthan retain some characters specific of flexible macromolecules. Indeed, were they rigid rods, the correlation length should remain equal to the rod length whatever the concentration.[8]

Materials

The aqueous xanthan solutions were made available to us by the Institut Français du Pêtrole. Xanthan is a stiff polysaccharide chain, obtained in the form of a fermentation broth from Rhône-Poulenc. Since it has a tendency to form aggregates and/or microgels, it was necessary to perform a careful filtration through Nuclepore filters just prior to use. A stock solution of 960 ppm was prepared at pH 7.0 in 0.1 M NaCl and was subsequently diluted to yield four samples at respectively 6, 96, 320, and 960 ppm. All solutions were protected from bacterial and oxidative degradation by the addition of 400 ppm sodium azide. They were observed to be stable over periods of several weeks. The average molecular weight was 1.8×10^6, with a polydispersity index M_w/M_n of 1.35. A precise characterization of our particular batch had been performed independently by Muller et al. using viscometry and static and quasi-elastic Rayleigh light scattering.[9] They model the xanthan chains as semiflexible monohelical rods of persistence length $q = 50 \pm 2$ nm and molecular diameter $d = 1.9$ nm. With a linear mass density of $M_L = 10^3$ daltons/nm, its contour length L_c is calculated to be 1.8 μm. The end-to-end distance L can be derived from the Porod–Kratky formula $L^2 = 2qL_c - 2q^2(1 - e^{-L/q})$.[10] With the above values for q and L_c, we get $L = 418$ nm. By comparison the end-to-end distance for a random coil of uncorrelated monomers and of similar molecular weight would be a low 60 nm, even accounting for some bond angle restriction.[11] On the other hand, xanthan is certainly not fully rigid since L is much lower than L_c. Viscosity data by Holzwarth on molecular fractions give an intrinsic viscosity–molecular weight exponent

0024-9297/86/2219-0085$01.50/0

of 0.96 for molecular weights larger than 10^6.[12] This is also strongly suggestive of some chain flexibility. The exponent value is intermediate between the theoretical value of 2 for a rigid rod and the experimental data of 0.70 for the flexible polyacrylamide and polystyrene chains.[13]

The xanthan chains were covalently labeled with fluorescein markers according to the procedure described by de Belder and Wik.[13] Isocyanide coupling was used to attach fluoresceinamine to the carboxylic groups of xanthan. 5-Aminofluorescein, acetaldehyde, and cyclohexyl isocyanide (reagent grade) were allowed to incubate in a dimethyl sulfoxide–water solution of xanthan at room temperature for several hours. The labeled polysaccharide was then purified by precipitation with ethanol and extensively dialyzed against 0.5% sodium chloride. The extent of dye labeling was determined by visible absorption spectrometry. The partial molar chromophore concentration was found to be 0.15% by weight. Their distribution is supposed to be at random along the chain.

Experimental Procedure

The experimental setup has been described in detail elsewhere.[14] A system of rotating mirrors allows one to vary the angle of incidence θ of a laser beam impinging on the solid–liquid interface formed by a fused-silica prism (optical refractive index $n_1 = 1.436$) and the xanthan polymer solution (refractive index $n_2 = 1.33$). If the laser beam propagates from the optically denser medium, it will experience total reflection for all angles θ larger than $\theta_c = \arcsin(n_2/n_1) = 67.85°$. There is nevertheless a penetration of the electromagnetic wave into the rarer medium, with exponentially decaying intensity over a distance $\Lambda = \lambda_0/4\pi n_1(\sin^2\theta - \sin^2\theta_c)^{-1/2}$. This evanescent wave is then used to excite the fluorescence of the labeled polymer chains onto specific distances. Variations of θ from θ_c to $\pi/2$ (glancing incidence) allows Λ to be tuned between ∞ and 70 nm (using $\lambda_0 = 488$ nm). The detected intensity is the integrated product of the energy of the evanescent wave times the chromophore concentration profile $\Phi'(Z)$. If the chromophores are randomly distributed along the chain, $\Phi'(Z)$ can be assumed to be a faithful image of the monomer concentration profile $\Phi(Z)$. Therefore

$$I_F^{pol} \simeq \int_0^\infty \Phi(Z) \exp(-Z/\Lambda)\, dZ \qquad (1)$$

All numerical factors related to the particulars of the experiment (collection efficiency of the fluorescence light, quantum yield of the detector, etc.) can be forgotten here since it is always possible to perform a relative instead of an absolute experiment. For this purpose, the intensity data of the labeled polymer solution are divided with the corresponding data obtained for a solution of unlabeled polymer mixed with free fluorescent markers at the same nominal concentration. In that latter case, the low molecular weight markers experience only very short-range repulsion with the wall and therefore $\Phi(Z)$ is uniform throughout the sample. Therefore $I_F^{ref} \simeq \Phi_b\Lambda$. The important point is that, if the experimental setup is kept unchanged, the prefactors are the same as before and the ratio I_F^{pol}/I_F^{ref} can be written as an equality

$$R(\Lambda) = (1/\Phi_b\Lambda)\int_0^\infty \Phi(Z) \exp(-Z/\Lambda)\, dZ \qquad (2)$$

Note that $\Lambda R(\Lambda)$ is just the Laplace transform of $\Phi(Z)$ vs. Λ^{-1}.

We have mentioned in ref 6 that the surface imperfections of the fused-silica substrate create a spurious volume excitation at all incidence angles. The effect is particularly conspicuous for $\theta > \theta_c$, where the signal due to the evanescent wave is weak. To obviate this problem, all the present experiments were performed on three different sample thicknesses $d = 50$, 100, and 250 μm. The intensity data obtained at each angle were then extrapolated to zero sample thickness. This procedure automatically cancels the parasitic contribution, which is a linear function of the thickness, whereas the evanescent wave contribution is independent of this parameter ($\Lambda \ll d$).

The excitation of fluorescence was from an Ar^+ CW laser at 488 nm. The light power at the sample level was of the order of 2 mW over a circular spot of 20 mm^2. The beam polarization was in the plane of incidence. The fluorescein emission was detected at 510 nm through an interference filter in front of a low dark-count phototube (Hamamatsu, R 549). Typical sample count rates were 400 counts per second at the lowest polymer concentration of 6 ppm and were of course much larger at higher concentrations.

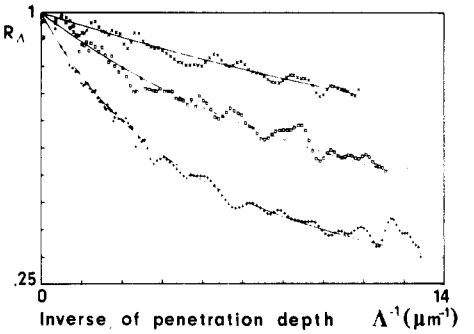

Figure 1. Fluorescence intensity ratio $R = I_F^{pol}/I_F^{ref}$ vs. the inverse of the penetration length of the evanescent wave Λ^{-1}. Xanthan polymer concentration is 96, 320, and 960 ppm. The data have been extrapolated to zero sample thickness (see text). The lines correspond to the best fits with a "rigid then flexible" profile, assuming a persistence length $q = 50$ nm.

Results

Figure 1 shows the fluorescence intensity ratios, R, as a function of the inverse of the penetration length, Λ, for three different bulk polymer concentrations Φ_b (96, 320, and 960 ppm). Data were also obtained with the 6 ppm solution. However, they are very noisy, due to the low fluorescence light levels involved. Since they fall onto the same curve as the 96 ppm, they have not been represented here. All three sets of data start from unity at the critical angle θ_c (i.e., $\Lambda^{-1} = 0$) and decrease monotonously as Λ^{-1} is increased. This is a clear signature for the existence of a depletion layer in the case of xanthan chains in contact with a nonadsorbing silica wall. As regions closer and closer to the wall (large Λ^{-1}) are probed, the density of monomers gets lower and lower and therefore the signal decreases relative to that of the uniform reference solution. Such behavior has already been observed in ref 5 and 6 and we provide here a mere confirmation. The most important point is that the amplitude of the signal decrease is a function of the bulk polymer concentration. This decrease is markedly reduced at the highest concentrations. Conversely, for any given Λ, R increases with Φ_b. This means that for a fixed irradiation volume (characterized by Λ) the average density of monomers within this volume increases with the bulk polymer concentration.

It is possible to make this statement more quantitative by using the properties of the Laplace transform. Since $R(\Lambda)$ is the Laplace transform of $\Phi(Z)$ it is easy to show that the derivative of R with respect to Λ^{-1} is a direct function of the surface excess $\Gamma = \int_0^\infty[\Phi(Z) - \Phi_b]\, dZ$ when $\Lambda^{-1} \to 0$. Indeed eq 2 for $R(\Lambda)$ can be rewritten as

$$R(\Lambda) = 1 + (1/\Phi_b\Lambda)\int_0^\infty [\Phi(Z) - \Phi_b] \exp(-Z/\Lambda)\, dZ \qquad (3)$$

Taking the derivative and considering the limit $\Lambda^{-1} \to 0$, we get

$$\left.\frac{dR}{d(\Lambda^{-1})}\right|_0 = \frac{\Gamma}{\Phi_b} \qquad (4)$$

The ratio Γ/Φ_b has the dimension of a length, which is customarily called the mean depletion layer thickness, e. Note that e, as defined by eq 4, is completely *independent* of the specific model for $\Phi(Z)$. In the case of a depletion layer, $\Phi(Z)$ is lower than Φ_b for $Z < e$ and the surface excess is negative.

In Figure 2, we have plotted the initial slope of our experimental curves $R(\Lambda^{-1})$ as a function of Φ_b. We note

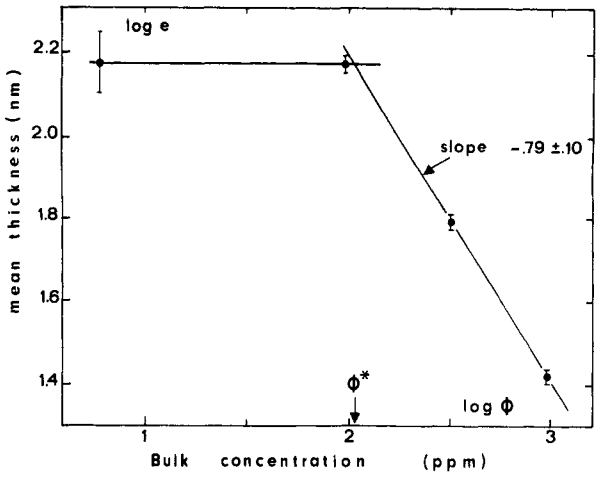

Figure 2. Semilogarithmic plot of the mean depletion layer thickness $e = \Gamma/\Phi_b$, as deduced from the initial slope of R vs. Λ^{-1}, vs. the bulk polymer concentration Φ_b. The straight line has a slope of 0.79, in agreement with the de Gennes prediction.

that it stays constant for the two lowest concentrations of 6 and 96 ppm and decreases markedly for 320 and 960 ppm. The data points at the two highest concentrations are compatible with a power law $e \sim \Phi_b^{-0.79\pm0.10}$, where $e = (1/\Phi_b)\int_0^\infty[\Phi(Z) - \Phi_b]\,dZ$. The crossover concentration between the two regimes can be estimated from the extrapolation of the two asymptotic curves to be $\Phi_b^* \simeq 105$ ppm.

Discussion

To the best of our knowledge, ref 3 is the first theoretical approach in the literature that predicts a variation of the polymer concentration profile in the interfacial region with bulk concentration. It applies to the case of semidilute solutions of flexible chains. In such cases, the authors have shown that the characteristic layer thickness is no longer the chain radius of gyration but the correlation length $\xi(\Phi_b)$. For good solvent conditions, ξ decreases upon increasing Φ_b as $\xi \sim \Phi_b^{-0.75}$. For ideal solvents, ξ varies as Φ_b^{-1}. The analytical profile predicted by mean-field arguments for semidilute solutions is $\Phi(Z) = \Phi_b \tanh^2(2^{1/2}Z/\xi)$, which becomes $\Phi(Z) = \Phi_b \tanh^2(Z/e)$ with $e \propto R_G$ in dilute solutions. Scaling arguments give slightly different predictions, but the differences between the two approaches are relatively subtle as far as the present experiments are concerned. The main point to bear in mind is that the mean depletion layer thickness e calculated from $e = \Gamma/\Phi_b$ should become proportional to ξ.

The main features of these theories are strongly supported by our results. e is observed to be independent of Φ_b below a critical concentration Φ^* (dilute regime) and to decrease strongly when Φ_b increases above Φ^* (semidilute regime). Quantitative statements are made difficult by the limited number of data points available. However, the variation seems compatible with a scaling law $e \sim \Phi_b^{-x}$, where $x = 0.79 \pm 0.1$. That value is comparable with the theoretical exponent in good solvent conditions ($x = 0.75$).

It is truly unfortunate that only two of our data points fully belong to the semidilute regime. Going to higher bulk concentrations was limited by the existence, around 2000 ppm, of a transition toward a macroscopically oriented, liquid crystalline solution. This anisotropic phase has of course completely different properties from the isotropic solutions considered here and is clearly beyond the scope of this work.[16]

On the other hand, we observe that the 96 ppm solution is just on the borderline between the dilute and the semidilute regimes. This correlates with the observations of Jamieson et al.[16] From their viscosity and quasi-elastic light scattering measurements, these authors were able to locate the crossover concentration around 250 ppm. The concentration of first overlap can also be calculated approximately from the relation $[\eta]\Phi_b^* = 1$, where $[\eta]$ is the intrinsic viscosity. Since $[\eta]$ has been measured to be 4.300 $cm^3\ g^{-1}$,[17] we expect $\Phi^* \simeq 200$ ppm, as indeed observed here. This low value for Φ^* is not too surprising if one considers the fact that the chain stiffness increases the overall chain dimension relative to that for a flexible chain of equivalent molecular weight. Taking $\Phi^* = (3/4\pi R_G^3)(M_w/\mathcal{N})$, where R_G is the chain radius of gyration and $\mathcal{N}$ the Avogadro number, one expects Φ^* to be 170 ppm if $R_G = L/7^{1/2} = 160$ nm.

It may look surprising at first sight to claim that we have observed a behavior typical of flexible chains with xanthan chains. It must however be realized that although the chain as a whole has been viewed in some instances as a rigid rod, it only has a finite persistence length. The present experiments exclude the possibility of xanthan being fully rigid. As pointed out by Auvray, the depletion layer thickness for a system of rods is independent of the bulk concentration as long as the solution stays isotropic.[8] It is true that the rotational and translational motions are impeded when the hydrodynamic volume swept by each individual rod is larger than the hydrodynamic volume swept by each object. However, the correlation length remains constant at the rod length L. Therefore the thickness of the layer affected by the wall should also be of the order L, whatever the bulk concentration. Such a behavior is clearly not observed here. This contradicts the representation of xanthan molecules as rigid rods with an equivalent rod length L smaller than the curvilinear length L_c. A much better description is that of a flexible coil with a low number of statistical units.

This last remark allows us to eliminate the ambiguity that was left in the data interpretation in ref 6 for the same xanthan solution at a single bulk concentration of 96 ppm. At that time, the data points could be fitted either with the Auvray profile for rigid rods or with a mixed "rigid then flexible" profile. Only this second model is compatible with the dependence of the mean depletion layer thickness on bulk concentration which is observed here. Xanthan macromolecules should then be viewed as Kuhn chains of freely jointed elements of length equal to twice the persistence length q. They behave as stiff rods for all distances to the wall smaller than $2q$ and as flexible coils for all distances larger than $2q$.

These remarks lead us to the interesting point that as Φ_b is gradually increased, $\xi(\Phi_b)$ and then the depletion layer thickness e will eventually become smaller than $2q$. In that case, the solution should behave in the interfacial region as a system of true rigid rods. One should therefore observe that e reaches a plateau as Φ_b is increasing. This is currently being checked with salt-free solutions of xanthan. Because of the additional electrostatic stretching,[11] this system has a larger persistence length. The saturation should then be observable at a lower bulk concentration Φ_b.

The only other case where the depletion layer has been considered experimentally is found in the work of Chauveteau et al.[18] on the effective viscosity of polymer solutions through small pores of radius R and with repulsive walls. Working also with xanthan solutions, they observed that the measured viscosity was considerably smaller (by a factor up to 4), than the viscosity of the same solution in an unbounded medium. They could rationalize their data by a coaxial flow model. The annular region of width δ

is supposed to contain a depleted solution at a fixed concentration Φ_{wall} while the central core of diameter $2(R - \delta)$ contains the solution at the bulk concentration Φ_b. the model has thus two adjustable parameters δ and $\beta = \Phi_{wall}/\Phi_b$, where β is the normalized average concentration of chains within a distance δ away from the wall. The experiments were performed on solutions of various concentrations up to 1500 ppm flowing through glass beads and sand packs. The data points could be fitted reasonably well with the rodlike Auvray model by taking $\delta = 0.7L$ and $\beta = 0.64$. L is the equivalent dynamic rod length as measured from intrinsic viscosity data and was fixed at 820 nm. Despite the success of the model to explain their data, it must be emphasized that contrary to the present observations, no concentration dependence could be detected through the parameters δ and β. The EWIF technique has the clear advantage of allowing the direct observation of the depletion profile. Therefore we believe that the concentration dependence of the profile is now established without ambiguity.

Conclusion

The present experiments show that the interfacial depletion layer that exists in polymer solutions in contact with a nonadsorbing wall is a function of the bulk polymer concentration Φ_b. For large enough concentrations, the mean depletion layer thickness e seems to scale with Φ_b as $\Phi_b^{-0.79}$. This is consistent with the de Gennes picture for flexible coils according to which e is proportional to the correlation length $\xi(\Phi_b)$ in the bulk. In dilute solutions, e is independent of Φ_b. We have shown earlier that in that case e is comparable to the end-to-end chain distance (or equivalently to its radius of gyration).

The present data support the view that xanthan chains, because of their finite persistence length, much larger than the monomer size but at the same time much smaller than the contour length L_c, exhibit a remarkable mixture of flexible and rodlike chain properties. The concentration dependence of e is definitely of flexible character since no such dependence is expected in the rod case. However, we have seen in ref 6 that the monomer concentration profile in the interfacial layer can by no means be described as that of a fully flexible chain and retains some rodlike behavior. There are two characteristic lengths, one associated with the chain end-to-end distance and the other with the local rigidity. This dual character has been mostly neglected in the more macroscopic experiments described by the previous workers.

Acknowledgment. This work has been supported by the Centre National de la Recherche Scientifique under an ATP "Polymères aux Interfaces" 070542. D.A. has benefited from a research scholarship from Elf-Aquitaine.

Registry No. Xanthan gum, 11138-66-2.

References and Notes

(1) See, for example: Casassa, E. F. *Macromolecules* **1984**, *17*, 601. Barnett, V. G.; Cosgrove, T.; Vincent, B.; Sissons, D. S.; Cohen-Stuart, M. *Macromolecules* **1981**, *14*, 1018.
(2) Hommel, H.; Legrand, P.; Tougne, P.; Balard, H.; Papirer, E. *Macromolecules* **1984**, *17*, 1578.
(3) Joanny, J. F.; Leibler, L.; de Gennes, P.-G. *J. Polym. Sci., Polym. Phys. Ed.* **1978**, *17*, 1073.
(4) See the reviews by: Vincent, B. *Adv. Colloid Interface Sci.* **1974**, *4*, 193. Takahashi, A.; Kawaguchi, M. *Adv. Polym. Sci.* **1982**, *46*, 1.
(5) Allain, C.; Ausserré, D.; Rondelez, F. *Phys. Rev. Lett.* **1982**, *49*, 1694.
(6) Ausserré, D.; Hervet, H.; Rondelez, F. *Phys. Rev. Lett.* **1985**, *59*, 1948.
(7) Asakura, S.; Oosawa, F. *J. Chem. Phys.* **1954**, *22*, 1255.
(8) Auvray, L. *J. Phys. (Les Ulis, Fr.)* **1981**, *42*, 79.
(9) Muller, G.; Lecourtier, J.; Chauveteau, G.; Allain, C. *Makromol. Chem., Rapid Commun.* **1984**, *5*, 203.
(10) Yamakawa, H. "Modern Theory of Polymer Solutions"; Harper and Row: New York, 1971.
(11) Wellington, S. L. *Polym. Prepr. (Am. Chem. Soc., Div. Polym. Chem.)* **1981**, *22*, 63.
(12) Holzwarth, G. *Carbohydr. Res.* **1978**, *66*, 173.
(13) de Belder, A. N.; Wik, K. O. *Carbohydr. Res.* **1975**, *44*, 251.
(14) Hervet, H.; Ausserré, D.; Rondelez, F. "Proceedings of the 27th IUPAC meeting on Macromolecular Dynamics"; Sedlacek, E., Ed.; Walter de Gruyter: New York, 1985; p 485–492.
(15) Fleer, G. J.; Scheutjens, J. H. M. H.; Vincent, B. *A.C.S. Symp. Ser.* **1984**, *240*, 245.
(16) Jamieson, A. M.; Southwick, J. G.; Blackwell, J. *J. Polym. Sci., Polym. Phys. Ed.* **1982**, *20*, 1513.
(17) Chauveteau, G. *J. Rheol. (N.Y.)* **1982**, *26*, 111.
(18) Chauveteau, G.; Tirrell, M.; Omari, A. *J. Colloid Interface Sci.* **1984**, *100*, 41.